INTERNATIONAL JOURNAL FOR NUMERICAL AND ANALYTICAL METHODS IN GEOMECHANICS
Int. J. Numer. Anal. Meth. Geomech., 2001; **25**:243–262

Three-dimensional finite element analysis of lined tunnels

C. E. Augarde*,† and H. J. Burd

**Department of Engineering Science, University of Oxford, Parks Road, Oxford, OX1 3PJ, U.K.*

SUMMARY

This paper describes finite element procedures that have been developed to model the ground movements that occur when a shallow tunnel is installed in a clay soil. This study is part of a wider project concerned with the development of new methods to predict the likely extent of damage to surface structures caused by nearby shallow tunnelling. This particular paper, however, is concerned only with the numerical model of tunnel installation. The structural liner is an important component of this tunnel installation model; two different ways of modelling the liner (based on continuum elements and shell elements) are discussed in the paper. A test problem consisting of the installation of a lined tunnel in an elastic continuum is used to investigate the merits of these different approaches. When continuum elements are used to model the liner, the numerical results agree well with an analytical solution to the problem. When shell elements are used to model the liner, however, the results were found to be significantly influenced by the particular formulation adopted for the shell elements. Example analyses, involving incremental tunnel construction in a clay soil where the soil is modelled using a kinematic hardening plasticity model, are described. These analyses confirm that a thin layer of continuum elements may be used, satisfactorily, to model tunnel linings in a soil–structure interaction analysis of this sort. Copyright © 2001 John Wiley & Sons, Ltd.

KEY WORDS: finite elements; tunnels

1. INTRODUCTION

There is increasing interest and activity in the construction of road or rail tunnels in urban areas for the improvement of transportation infrastructure. These tunnels are generally relatively shallow and there is, therefore, a risk that ground movements occurring during construction may cause damage to existing buildings on the soil surface.

Current design methods for the assessment of buildings at risk of settlement-induced damage are often based on a two-stage process. In this procedure an assessment of likely surface settlements at an equivalent 'greenfield' site (where buildings are absent) is first carried out, usually by means of a semi-empirical approach [1]. Secondly, the effect of these settlements is

* Correspondence to: C.E. Augarde, Department of Engineering Science, University of Oxford, Parks Road, Oxford, OX1 3PJ, U.K.
† E-mail: charles.augarde@eng.ox.ac.uk

Received 11 January 2000
Revised 10 August 2000

assessed by applying them to structural models of any nearby buildings to estimate the likely extent of any damage. This procedure neglects the important effect that the building's own stiffness and weight has on the shape and magnitude of the settlement profile and it is well accepted that this may lead to inaccurate predictions.

The alternative of using numerical analysis to study this problem has the advantage that, in principle, the building and the tunnelling process can be included in a single model; interaction effects between the building and the soil are therefore specifically included in the analysis. These interaction mechanisms are highly complex, however, and can only be modelled in detail using three-dimensional procedures [2–4]. Much of the previous numerical modelling of this problem, however, has been based on two-dimensional models [5–7] which lead naturally to problems of reduced complexity. Continuing developments in computer hardware and numerical algorithms for the solution of large systems of linear equations, however, mean that three-dimensional numerical studies of this problem are now becoming a realistic practical possibility [8].

This paper describes some of the development work that has been carried out on a three-dimensional finite element model to assess the extent of likely damage caused to a masonry structure on the soil surface by nearby shallow tunnelling procedures [2–4]. This model is capable of investigating problems of the sort illustrated in Figure 1 in which a tunnel is incrementally installed beneath an existing masonry building. The soil is modelled using tetrahedral elements, shell or tetrahedral elements are used to model the tunnel lining and the building consists of sets of interconnected facades of plane stress elements. This paper describes the procedures used to model tunnel installation procedures and discusses the relative merits of using shell and tetrahedral continuum elements for the lining. Modelling procedures for the building [3,4] and for the non-linear behaviour of the soil [9] are described elsewhere and are beyond the scope of this paper.

2. MODELLING AN EMBEDDED TUNNEL LINING

The tunnel liner in this numerical model consists of a thin circular elastic tube embedded in the soil. A choice exists between two different approaches that may be used to model this liner. One

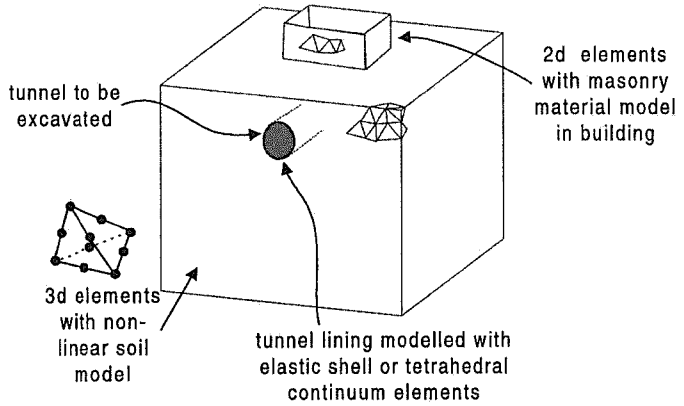

Figure 1. Example analysis of a building, soil and tunnelling process.

possibility is to use a thin layer of continuum elements. The other possible approach would be to use an appropriate shell element formulation (of which there are many) to model the liner. These two approaches are reviewed below.

2.1. Modelling the liner with continuum elements

The use of continuum elements to model the liner, as well as the soil, raises two important objections [10,11]. Firstly, more degrees-of-freedom are generally required than for an alternative approach in which specially formulated shell elements are used. This objection does not have any substance for the current problem, however, as the number of degrees-of-freedom used to model the tunnel liner is a small fraction of the number of degrees-of-freedom required to describe the complete problem. The second objection is that it inevitably involves the use of relatively stiff elements that have poor geometric conditioning [11]; this leads to an increased difference between the largest and smallest magnitude terms in the structure stiffness matrix. This increased range of magnitude of terms in the stiffness matrix tends to make the solution to the system of equations more susceptible to truncation and round-off errors occurring during the solution process. This increased susceptibility to numerical errors is referred to as 'ill-conditioning' and is generally associated with a large value of the condition number of the stiffness matrix. It is, however, far from straightforward in practice to discover whether any particular set of equations are ill-conditioned; indeed Neto [12] shows that a relatively large value of condition number is not, in itself, necessarily an indication of ill-conditioning. Truncation and round-off errors, however, can be reduced (at least in principle) by the use of higher precision arithmetic. The errors may also be sensitive to details of the solution process, such as the order in which the stiffness equations are assembled and solved.

In principle therefore, provided that any potential difficulties caused by ill-conditioning and round-off errors can be identified and dealt with, the use of conventional continuum elements would seem to be a reasonably practical way of modelling embedded tunnel liners. The use of conventional three-dimensional continuum elements has the further important advantage that numerical difficulties associated with the use of specially formulated shell elements (see below) are avoided.

In the analyses described in this paper, the soil is modelled using 10-noded tetrahedral elements. These elements have the important advantage for soil modelling that they are of a sufficiently high order to allow accurate modelling of incompressible material behaviour as would occur, for example, in a problem involving undrained soil behaviour [13]. Since the strain variation within these elements is linear, a single thin layer of elements, when used to model the tunnel liner, should provide a reasonable representation of the stress variations associated with both shell bending and membrane action.

2.2. Modelling the liner with shell elements

A variety of shell element formulations are proposed in the current literature; Yang *et al.* [14], for example, review over 280 relevant publications. Many of these formulations are highly complex because of the need to satisfy C^1 continuity at the element boundaries. These formulations may be grouped in two broad categories as described below.

2.2.1. Curved shell elements. Curved shell elements may be formulated directly by using a suitable shell theory. Formulations based on this approach generally require multiple

degrees-of-freedom at nodes. Some of these terms relate to high-order displacement derivatives and this can lead to conflicts because of their dependence on other lower-order terms, which are also degrees of freedom [15]. These conflicts may significantly reduce the accuracy and convergence performance of the element. An alternative approach is to start from the conventional isoparametric approach that is used for solid hexahedral elements. The displacement degrees of freedom at the element nodes are expressed in terms of translation and rotation degrees-of-freedom for an element with the same geometry but with a reduced number of nodes. Elements formulated in this way are often termed 'degenerated solid continuum elements'. This approach might typically be used to obtain an 8-noded shell element from a 20-noded isoparametric continuum element.

Curved shell elements have obvious appeal that they are able to model closely the geometry of a curved shell. They suffer from the important disadvantage, however, in that spurious coupling may exist between the membrane and bending response of the element. Since shell elements usually have a large membrane stiffness and a relatively small flexural stiffness, this coupling can lead to meshes in which the bending stiffness of the shell elements is artificially increased to unacceptably high levels. This phenomenon (known as 'membrane locking') is conventionally dealt with by various numerical procedures, including the use of reduced or selective integration, in the computation of the element stiffness matrix.

2.2.2. Faceted shell elements. Faceted shell elements consist of one, or more, plane facets. Elements of this sort have the important advantage that bending and membrane effects are uncoupled within each facet and this reduces the complexity of the formulation. This lack of coupling also avoids the problems associated with 'membrane locking'. Faceted formulations, however, are clearly unable to model the detailed geometry of a curved shell. No clear consensus yet appears to have emerged as to whether the advantages of this simpler formulation approach outweigh this disadvantage [10,16].

In most formulations of faceted elements, separate formulations must be selected for flexural and membrane behaviour. The membrane component is usually based on a conventional, plane stress, Lagrangian continuum element. Formulations for the flexural behaviour, however, require special consideration of the rotational degrees-of-freedom at the nodes. Simple formulations for flat bending elements (or plate elements) are based on three degrees-of-freedom at each node: one out-of-plane displacement and two rotations, as shown in Figure 2. A complete set of three rotational degrees-of-freedom per node is required, however, to formulate faceted shell elements that can be connected together to form a curved three-dimensional surface. This requires the introduction of a rotational degree-of-freedom (often referred to as the 'drilling degree of

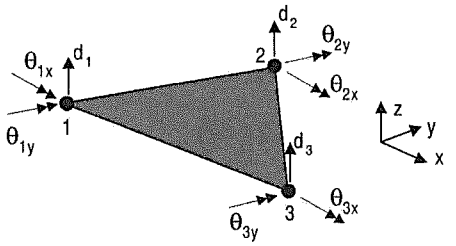

Figure 2. Degrees of freedom for flat-plate element.

freedom') in a direction normal to the element. Several formulations of membrane elements that include drilling degree of freedom stiffness terms [17–19] have been proposed and these could be used within a shell element formulation. Alternatively, a fictitious drilling degree-of-freedom stiffness can be placed in the element stiffness matrix [20].

A novel faceted element formulation is described by Phaal and Calladine [15]. This element is formulated in terms of displacement degrees of freedom only and as a consequence the drilling degree of freedom issue described above does not arise. The absence of rotational degrees of freedom also makes it attractive for use in problems where shell elements are combined with conventional displacement continuum elements.

2.3. Choice of element for the tunnel lining

This paper describes analyses carried out using a variety of approaches to modelling the tunnel liner. Some analyses were carried out using a thin layer of continuum elements to model the liner, and in the other calculations the liner was modelled using shell elements.

Two types of shell element are investigated. One of these is the faceted shell formulation proposed by Phaal and Calladine [15]. This element has been implemented in the finite element program OXFEM [2–4] that has been developed at Oxford University for the analysis of three-dimensional problems in geotechnical engineering. Test analyses have also been carried out, using the commercial program ABAQUS [21], in which an alternative shell element formulation is used for the liner.

The Phaal and Calladine element is based on the use of overlapping displacement fields; this formulation is reviewed briefly below. The curved shell element used in the ABAQUS analyses (referred to in ABAQUS [21] documentation as STRI65) is based on curved thin shell theory. This element is formulated in terms of three displacements and two rotations at each node. Additional fictitious stiffness terms associated with the 'drilling degree-of-freedom' are included to avoid the possibility of a singular stiffness matrix for the case where elements connected to any node lie in the same plane. A reduced integration scheme is used to avoid the possibility of 'membrane locking'.

3. THE PHAAL AND CALLADINE [15] ELEMENT

The Phaal and Calladine element consists of four plane facets, defined by the positions of six nodes, as shown in Figure 3(a). The membrane terms in the element stiffness matrix are obtained by assembling the individual stiffness matrices of conventional three-noded plane stress elements corresponding to each facet. The formulation for the flexural terms is more complex, however, and is based on a mesh of layers of overlapping elements (Figure 3(b)). The use of overlapping elements in this way allows for C^1 continuity without the need to introduce rotational degrees-of-freedom at the nodes. It does, however, lead to additional complexities in the formulation, particularly in the implementation of the boundary conditions. The formulation adopted for the flexural behaviour may be understood by taking a formulation for a flat plate element as a starting point. Phaal and Calladine propose a simple mechanical analogy for this plate element (consisting of rigid facets and rotational springs); this mechanical analogy is then used to develop a formulation for a curved version of this element.

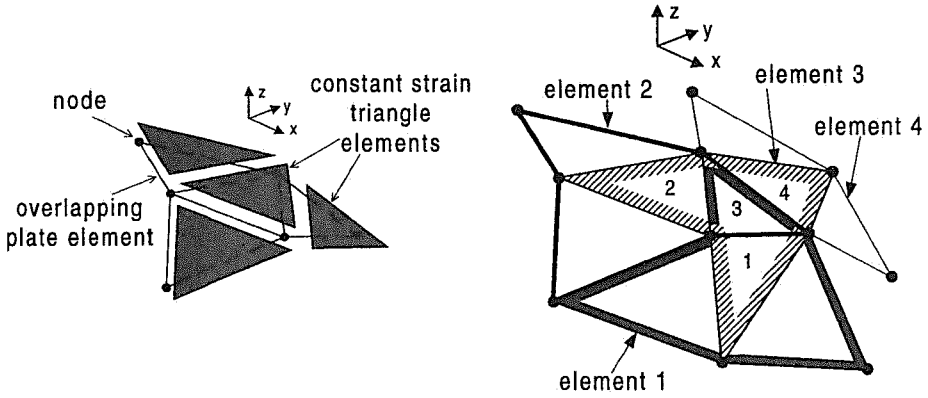

Figure 3. (a) Phaal & Calladine shell element [15]. (b) Mesh of overlapping shells.

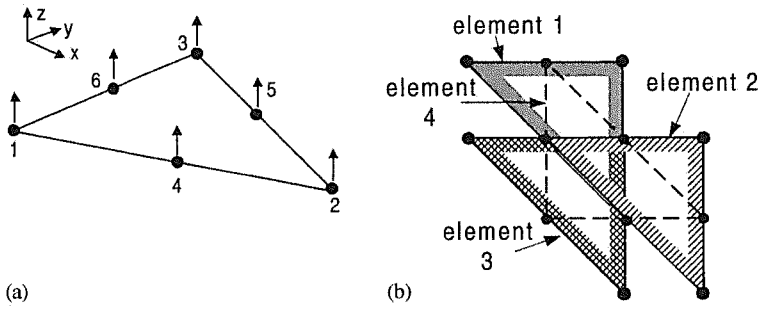

Figure 4. (a) Lagrangian plate element. (b) Overlapping mesh of Lagrangian plate element.

The formulation for the flexural behaviour of the shell element starts from a planar six-noded element (Figure 4(a)). This element is defined in terms of out-of-plane degrees of freedom only and conventional Lagrangian interpolation polynomials are used to relate the nodal displacements to the element curvatures. These elements may be assembled to form a mesh in which C^1 continuity is ensured by overlaying them, as shown in Figure 4(b). This procedure is a development of an approach described by Zienkiewicz and Morgan [22], who show that a mesh of overlaid one-dimensional Lagrangian elements leads to stiffness equations that are identical to those that would be obtained from a finite difference analysis of a beam.

Phaal and Calladine show that the same stiffness matrix for the six-noded flat plate element may be derived using a mechanical model consisting of four rigid facets connected together with three rotational springs of a suitable stiffness (Figure 5(a)). This mechanical model is significant because it may then be used to derive a curved element as described below.

The curved version of the mechanical shell model is developed by considering a faceted element in which the facets are connected together, at appropriate angular orientations, along the lines of the three rotational springs, as shown in Figure 5(b). The flexural behaviour of the element is described in terms of displacements at each node in a direction normal to each facet. (Note that nodes 1,2,3 have associated with them a single nodal displacement in a direction normal to the

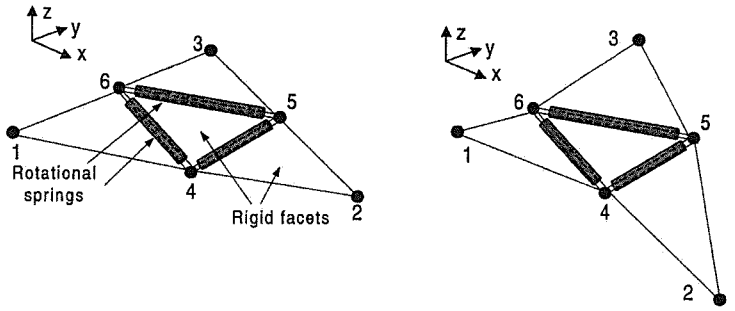

Figure 5. (a) Mechanical model of plate element. (b) Mechanical model of shell element.

connected facet. Nodes 4,5, and 6 have nodal displacements in three different directions associated with them because the three connecting facets will, generally, have normals in different directions). These 12 displacement degrees-of-freedom need to be expressed in terms of the 18 degrees-of-freedom (three per node) that are used to define the complete element. The procedures used to achieve this are described by Phaal and Calladine [15] and are not discussed further here.

Since the elements have no rotational degrees of freedom, special procedures are required to specify boundary rotations that are free or fixed. The approach proposed by Phaal and Calladine, and adopted in the formulation used for these analyses, is to modify the flexural terms in the stiffness matrices of elements at the edge of the mesh to specify the appropriate rotational boundary condition. Modifications are not required for the membrane stiffness terms. These procedures require special measures to be taken during mesh generation (to identify edge elements) and the stiffness matrix formation. The complexity of these procedures is regarded as a major disadvantage of this element.

4. TUNNELLING THROUGH AN ELASTIC MEDIUM

4.1. Test analyses

To investigate the performance of different procedures to model an embedded tunnel liner, a set of test analyses was carried out of the installation of a deep tunnel through a prestressed, elastic medium with no self-weight. This is a plane strain problem and so it does not involve bending along the tunnel axis. The problem does, however, have an analytical solution [22] and is therefore useful for testing purposes. Three meshes of different refinement were used in the study.

These test analyses were concerned with a tunnel installed in a cubic block of ground with sides of length 24R. The three meshes used in the analyses are shown in Figure 6(a). For analyses where continuum elements were used to model the liner a layer of continuum elements of thickness $0.1R$ was included as shown in Figure 6(b). For analyses where the shells were used to model the liner this thin ring of continuum elements was removed and replaced by shell elements. The numbers of elements used in each analysis are given in Tables I and II. One-quarter of the whole problem was

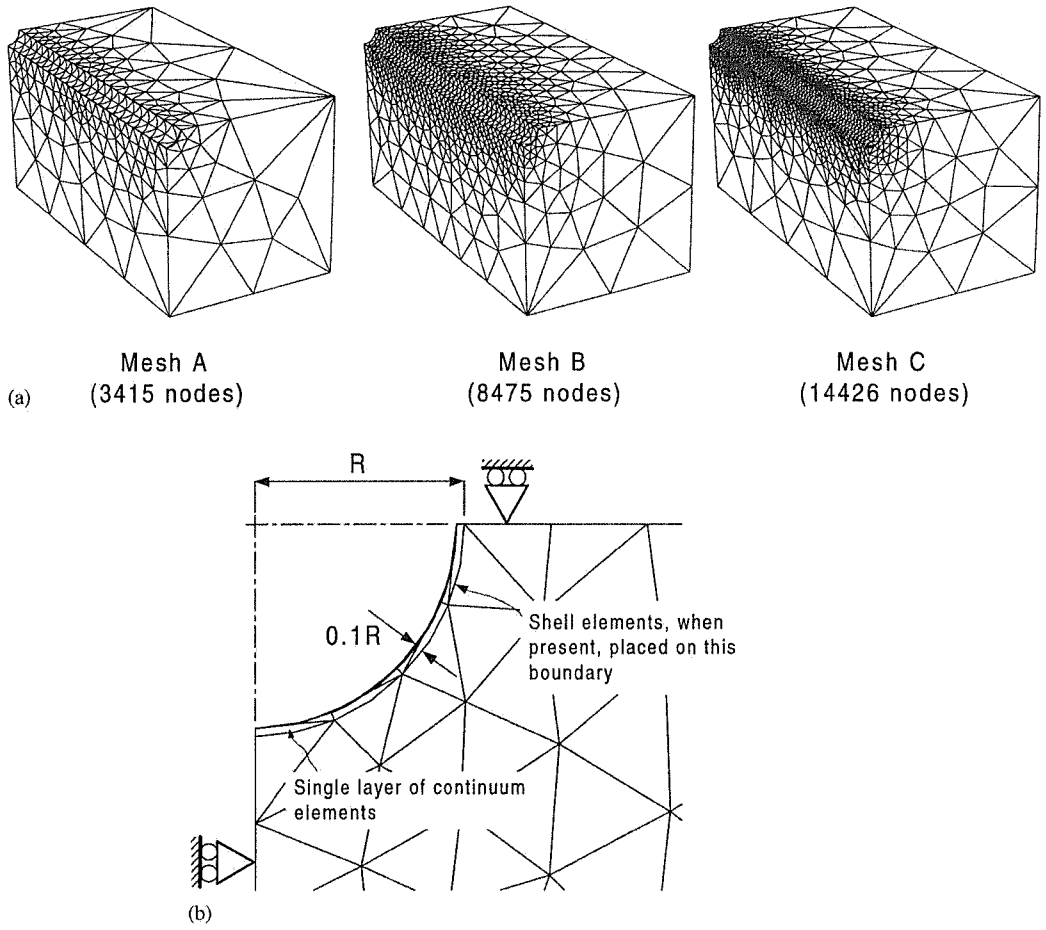

Figure 6. (a) Finite element mesh for tunnel installation in weightless elastic medium. (b) Tunnel liner details.

Table I. Mesh details for analyses of tunnelling through an elastic medium.

Mesh	No. of soil elements	No. of elements within excavated volume	No. of continuum elements to model liner (when present)	No. of shell elements (when present)
A	1263	222	296	376
B	3676	408	1025	960
C	6241	1325	1528	1905

modelled to take advantage of symmetry. Symmetric (zero rotation) boundaries for the overlapping shell elements were specified along both longitudinal edges of the tunnel lining mesh. Initial vertical and horizontal compressive stresses of σ and $K\sigma$ were assigned to the soil at the start of the analysis. In the results presented here, K was 0.8 and the soil Poisson's ratio was 0.49 (selected

Table II. Specification of analyses of tunnelling through an elastic medium.

Run	Mesh	No. of elements	No. of nodes	Lining element type
cl_A	A	1559	2682	Continuum
cl_B	B	4701	7873	Continuum
cl_C	C	7769	12627	Continuum
sl_A	A	1639	2179	Shell
sl_B	B	4636	6312	Shell
sl_C	C	8146	10325	Shell

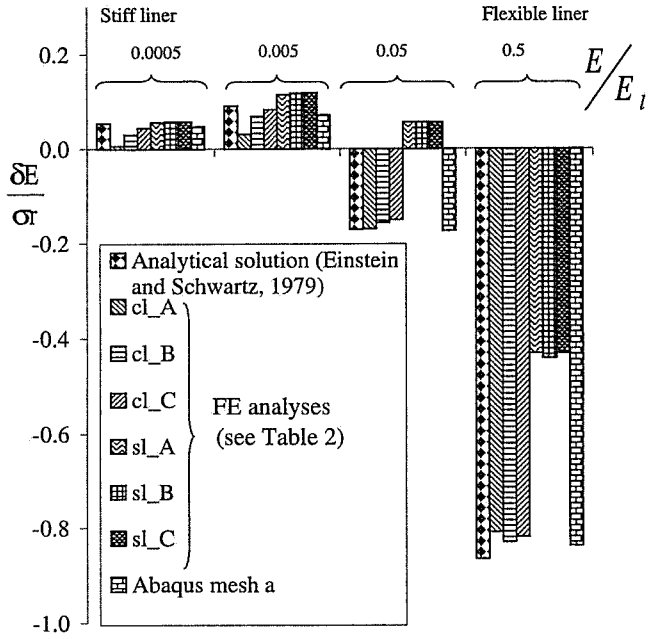

Figure 7. Comparison between computed liner displacements and solutions of Einstein & Schwartz [25] (springline).

to approximate an incompressible soil). Calculations were carried out with different values of E/E_l where E and E_l are the Young's moduli of the soil and the liner, respectively. The Poisson's ratio of the liner was 0.25.

Excavation was modelled by removal of the stiffness and self-weight contributions of the elements within the tunnel volume (these elements are not shown in Figure 6). Equilibrium on surfaces adjacent to excavated elements was ensured by using procedures described by Brown and Booker [23]. The implementation of these procedures is described by Augarde *et al.* [24].

The computed radial displacements on the springline and invert (averaged along the length of the tunnel) are compared with the analytical solutions of Einstein and Schwarz [25] in Figures 7 and 8. The displacements are shown in non-dimensionalized form where δ is radial displacement

and r, the tunnel radius, is equal to R when the lining is modelled by shell elements and $0.95R$ when modelled using continuum elements. The value of E/E_l clearly has an important influence on the liner displacements. For small values of this stiffness ratio, the liner behaves as a stiff tube and displacements are small. For larger values of E/E_l, the liner response is more flexible and displacements are larger. The displacements obtained from the OXFEM analyses based on the use of continuum elements to model the lining are similar to those obtained from the ABAQUS analysis; both sets of data agree well with the analytical solution. These data show that mesh refinement appears to have little effect on the results of the analysis when shell elements are used to model the tunnel lining. The use of refined meshes with the continuum element approach does, however, lead to convergence towards the analytical solution.

The results from the OXFEM analyses employing the Phaal and Calladine elements, however, show a different pattern. Although the computed displacements show trends that are similar to the analytical solution, the computed displacements are consistently in error by an amount that tends to increase as the liner becomes more flexible. The pattern of results suggests that the behaviour of the elements is over-stiff. It has already been noted that special measures are often needed to ensure that shell element formulations do not exhibit flexural behaviour that is excessively stiff. It is thought, therefore, that this particular element requires further development before it is suitable for accurate soil–structure interaction analyses of this sort. It should be noted in passing, however, that values of E/E_l appropriate for soft ground tunnelling are likely to be in the range 0.001–0.01, and in this range the Phaal and Calladine element appears to provide reasonable agreement with the analytical solution.

4.2. Element conditioning

The use of continuum elements to model the tunnel lining leads to relatively long and thin elements. The poor geometric conditioning may have an important influence on the solution, however, as discussed in Section 2.1.

The geometric condition of a tetrahedral element may be characterized by various measures [11]. One possible geometric condition number, ψ, is defined as

$$\psi = \sqrt{(24)}\,\frac{\text{radius of largest inscribed sphere within element}}{\text{longest edge of element}} \tag{1}$$

where the factor $\sqrt{(24)}$ ensures that ψ is unity for a regular tetrahedron. For the meshes used in this study, the continuum elements used to model the liner have a geometric condition number of about 0.17. To investigate whether this level of geometric ill-conditioning is likely to adversely effect the results, the analyses c1_A and c1_C were repeated using single-precision arithmetic (rather than the double-precision arithmetic that was used to compute the results plotted in Figures 7 and 8) for the real variables. The results for computed springline displacements, averaged along the length of the tunnel are compared with the equivalent double-precision analyses in Table III. The data show a small influence on calculation precision which is, presumably, due to increased truncation and round-off errors in the solution procedure when single precision arithmetic is used. It is interesting to note that the differences between the averaged displacements tend to increase with increasing stiffness ratio E/E_l. This is consistent with the expected pattern of truncation and round-off errors increasing with increasing difference in the stiffness of the liner and the soil. In general terms, however, the differences between the two sets of results suggest (although this cannot be confirmed) that any round-off errors caused by

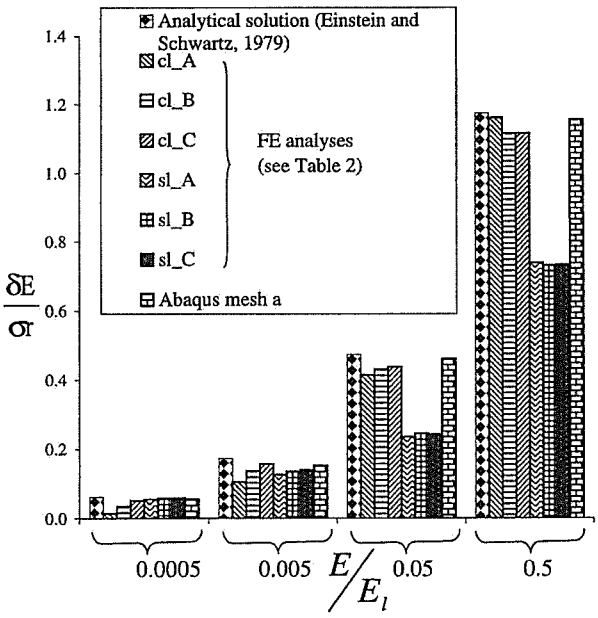

Figure 8. Comparison between computed liner displacements and solutions of Einstein & Schwartz [25] (invert).

Table III. Comparison of results of single and double precision analyses.

Analysis	E/El	Mean	Std. dev.	Mean	Std. dev.	in mean % diff.	in SD % diff.
cl_A	0.0005	0.304	0.312	0.301	0.310	1.11	0.60
	0.005	1.494	0.990	1.466	1.038	1.96	− 4.64
	0.05	− 7.998	0.871	− 7.984	0.878	− 0.18	− 0.77
	0.5	− 38.318	7.424	− 38.322	7.505	0.01	− 1.08
cl_C	0.0005	2.067	0.049	2.099	0.045	− 1.52	7.22
	0.005	3.940	0.221	3.964	0.215	− 0.60	2.64
	0.05	− 7.088	0.346	− 7.085	0.347	− 0.04	− 0.16
	0.5	− 38.780	0.594	− 38.792	0.595	0.03	− 0.24

poor geometric conditioning of the elements used to model the liner are minimal in the double precision analyses.

5. MODELLING TUNNEL INSTALLATION

In any practical tunnel construction the volume of soil actually excavated is larger than the final tunnel volume. This difference in volume is conventionally referred to as 'ground loss'. To model

real tunnel construction processes, therefore, it is necessary to develop a means of incorporating ground loss within the numerical analysis. In an ideal case the ground loss would be zero; in practice, however, values of ground loss of between 1 and 2 per cent (expressed in terms of the final tunnel volume) are typical. (Note that these values are dependent on the method of tunnel installation used and the quality of workmanship. In practice, ground loss values in excess of 2 per cent may occur.) The simulation of tunnel installation, including the effects of ground loss, is carried out in this numerical model as follows.

Excavation of material within the tunnel. This is carried out using the procedures described for the analyses in Section 4.

Activation of the lining. Lining elements in a previously generated mesh are activated.

Application of the required amount of ground loss. This is achieved by numerical shrinkage of the liner elements. These procedures are described in more detail below.

5.1. Modelling ground loss

Two important features of ground loss need to be considered; (a) loss associated with ground moving into the tunnel at the face (termed face loss) and (b) loss caused by radial movement of the soil prior to placement and grouting of the lining (termed tail loss). Face loss, in principle, is automatically included in the model since the numerical procedure includes the possibility of movements at the tunnel face. In practice these movements are often controlled using slurry shield or earth pressure balance techniques. Although these construction techniques are not included in the model described in this paper they could be incorporated by using suitable numerical procedures. Tail loss (which is usually more significant than face loss), needs to be specifically included in the analysis.

Three separate numerical procedures to model tail loss may be identified from previous work in this area. Bakker *et al.* [26] and El-Nahhas *et al.* [27], for example, use a two-dimensional approach in which beam elements (to model the lining) are connected to the mesh of continuum elements used to model the soil. To develop a specified amount of ground loss, the liner elements are simply subjected to a specified amount of circumferential shrinkage. An alternative two-dimensional approach is described by Addenbrooke and Potts [6], in which element removal within the tunnel volume is carried out in increments without including a specific model for the liner. At the end of each increment the volume loss is computed and, when it reaches the desired value, the calculation is simply terminated. A more complex approach is described by Rowe [28] in which separate unconnected meshes are adopted for the soil and the liner. The geometry of the liner mesh is devised so that the difference between the excavated area, and the area enclosed by the liner elements, is equal to the required amount of ground loss. During tunnel installation a soil–lining interaction formulation is used to model the closure of the ground onto the tunnel.

The methods described above have been implemented in two-dimensional analysis. Little work appears to have been done, however, on their possible extension to three-dimensional analysis. The extension of the 'shrinkage method' of Bakker *et al.* [26] and El-Nahhas *et al.* [27] and the 'partial unloading' method of Addenbrooke and Potts [6] to three dimensions would seem to be relatively straightforward. The interaction approach adopted by Rowe [28] appears to provide a more realistic model, but it would be highly complex to formulate in three dimensions. The tunnelling model described here was developed for the purpose of investigating surface settlements, and consequential damage to surface structures caused by tunnelling. Since for these

calculations a detailed study of liner performance was not required, it was thought that a relatively simple ground loss model would be acceptable. Accordingly a procedure similar to the shrinkage model described above was adopted. Although this procedure does not model the detailed soil–structure interaction in the neighbourhood of the tunnel, it does allow specified amounts of ground loss to be developed.

Shrinkage of the tunnel lining is achieved by applying an appropriate set of nodal forces to the tunnel lining. These forces are calculated on an element-by-element basis. For shell elements, the required nodal forces are obtained from a conventional virtual work approach to give

$$\mathbf{f}_{ax} = \int_A \mathbf{B}^T \mathbf{D} \varepsilon_1 \, dA \tag{2}$$

where $\mathbf{B}$ is the strain–displacement matrix, $\mathbf{D}$ is the material constitutive matrix element and ε_1 is the vector of strain components that correspond to the required amount of hoop shrinkage within the lining. A similar approach is used for continuum liner elements but the integration is carried out over the volume of each element. Since the liner is elastic, these forces do not modify the behaviour of the liner although they do lead to additional hoop stresses that have no physical significance.

6. EXAMPLE TUNNELLING ANALYSES

A set of example analyses have been carried out using OXFEM to illustrate the use of this tunnelling model. Two of these analyses were based on a lined tunnel and the third on an unlined tunnel. Details of these analyses are given below.

6.1. Soil model

The soil model was based on an elastic–plastic approach in which the plastic behaviour was modelled by multiple kinematic hardening yield surfaces. Stiffness and strength were specified to increase with depth. This soil material was developed to model the small strain non-linearity that is known to have an important influence on the response of overconsolidated soils [9]. Non-linearity of the small strain response is achieved using a number of nested von Mises surfaces which translate according to a linear hardening model. The model includes an outer von Mises bounding surface. The initial shear modulus at the surface of the mesh, G_0 was 30000 kPa and the increase with depth was 3000 kPa/m. Figure 9 shows the variation in shear modulus with shear strain for a point at a depth of 10 m from the surface with this material model. A value of 0.8 was adopted for K_0. Undrained behaviour was approximated by setting Poisson's ratio, $\nu = 0.49$. The initial stresses in the soil were determined by taking the bulk unit weight of the soil to be 20 kN/m^3 and assuming the water table to lie at the surface. A Young's modulus of 30 kN/m^2 and Poisson's ratio of 0.2 were used for the lining; these are consistent with the values normally assumed for reinforced concrete. The membrane and flexural properties for the lining were derived from these values and an assumed thickness of 250 mm.

6.2. General arrangement for the analyses

In all analyses, the tunnel axis was straight, horizontal and at a depth of 10 m and the tunnel inside radius was 2.5 m. The mesh (in which the symmetry of the problem is exploited) is shown in

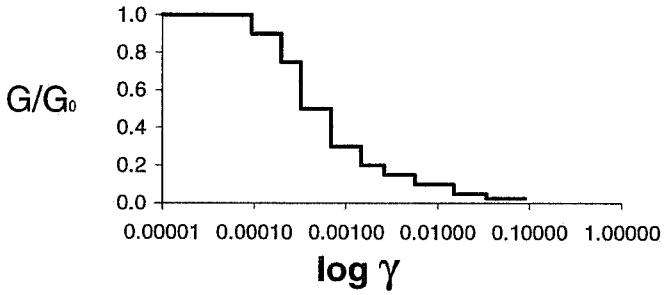

Figure 9. Variation of shear modulus with shear strain.

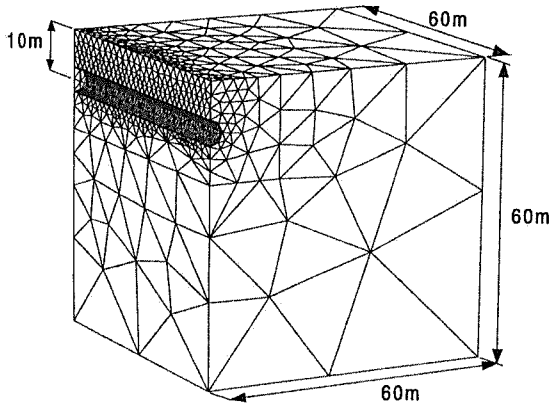

Figure 10. Finite element mesh used for example tunnelling analysis.

Figure 10 and the three analyses are specified in Table IV. Details of the way in which the lining (where present) was modelled follows a similar pattern to that shown in Figure 6(b) with $R = 2.5$ m. For the analysis in which the liner was modelled using continuum elements (CL) an elastic model with the appropriate liner properties was assigned to a 0.25 m thick layer of tetrahedral elements around the tunnel perimeter. For the unlined analysis (UL) this thin layer was removed. In the third analysis (SL), the thin continuum element layer was absent and shell elements were placed around the inside tunnel at a radius of 2.5 m. In analyses CL and SL the ground loss was specified to be 1 per cent; in the unlined analysis, however, ground loss could not be controlled. The tunnel was excavated in 10 equal stages, each 6 m long. At the end of each analysis stage the volume of the tunnel was calculated (by a three-dimensional triangulation within the tunnel) to calculate the amount of ground loss that was actually developed; these data are given in Table IV. For the lined tunnels the developed ground loss is very close to the specified value of 1 per cent. (The difference between specified and actual ground loss is presumed to be associated with ground loss at the tunnel face). The use of symmetrical boundary conditions on the vertical faces of the mesh implies that another tunnel is simultaneously constructed, in the opposite direction, to meet the final stage of the analysis. The effect of this is to slightly over-estimate the settlements as the tunnel reaches the far face of the mesh.

Table IV. Example analyses specifications.

Analysis Reference	Lined/unlined	No. of elements	No. of nodes	Ground loss specified (%)	Ground loss measured (%)	Equivalent trough width parameter, i (m)
UL	Unlined	6476		N/A	2.66	7.12
SL	Lined (overlapping shell elements)	7436	9735	1.0	1.13	9.70
CL	Lined (continuum elements)	6476		1.0	1.17	7.39

6.3. *Empirical prediction of settlements*

The analyses presented here are for a greenfield site and may therefore be compared with surface settlements estimated using the standard semi-empirical approach [1]. In this procedure the transverse profile of settlement is assumed to follow the Gaussian curve

$$S = S_{\max} e^{-x^2/2i^2} \tag{3}$$

where $S_{\max}$ is the maximum settlement above the tunnel axis and x is the transverse distance from the tunnel axis. The width of the settlement trough is defined by the parameter i which varies according to the depth of the tunnel and the nature of the ground. For overconsolidated clays, the relation $i = 0.5Z$, where Z is the depth to the tunnel axis, is often assumed [1].

In this semi-empirical approach, the longitudinal profile of the surface settlement is assumed to follow the cumulative Gaussian curve

$$S(y) = \frac{S_{\max}}{2}\left[\operatorname{erf}\left(\frac{y - y_f}{i\sqrt{2}}\right) - \operatorname{erf}\left(\frac{y - y_s}{i\sqrt{2}}\right)\right] \tag{4}$$

where y is the co-ordinate along the tunnel axis, y_f is the current location of the tunnel face, y_s is the starting point of the tunnel excavation. (Note that for the case of a tunnel whose excavation begins a large distance from the face, the second error function term tends to unity.)

6.4. *Prediction of settlements from the numerical model*

Figure 11 shows the computed transverse settlement profile at the centre of the mesh (i.e. $y = 30$ m) for various stages of the unlined analysis (UL). Similar plots for the lined analyses are shown in Figures 12 and 13. Also plotted are the settlement profiles obtained from Equation (2) with $i = 5$ m and taking the appropriate value of ground loss from Table IV. Note that in these plots r is the appropriate value for tunnel radius, which is 2.5 m for runs UL and SL and 2.375 m for run CL.

These plots show the gradual development of transverse settlement as the tunnel progresses. At the end of the analysis (stage 10) all three analyses show a well-defined settlement trough above the tunnel. As expected, the magnitude of the settlements for the lined analysis are generally less than those from the unlined analysis.

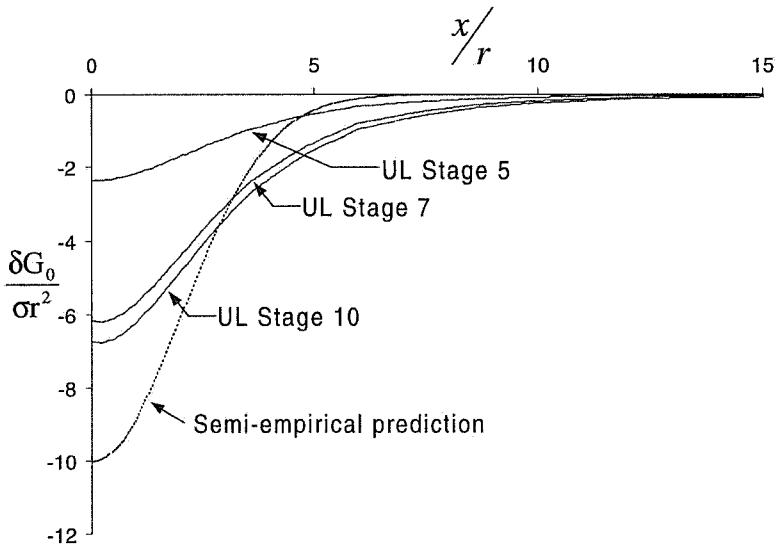

Figure 11. Transverse settlement profile (UL).

For all three analyses the computed variation of settlement with distance from the tunnel axis are similar in shape to a Gauss curve, but the computed settlement troughs are clearly wider (and the maximum settlement correspondingly smaller) than the semi-empirical predictions. Table IV lists values of 'equivalent trough width parameter' which correspond to a Gauss curve with values of maximum displacement and ground loss taken from the numerical analyses. These width parameters are rather larger than the value of 5 m that would be expected for a tunnel at 10 m depth in overconsolidated clay. This overprediction of settlement trough width is, in fact, a common feature of tunnelling analysis. Stallebrass *et al.* [29], for example, noted a similar effect when using a multiple yield surface model to back-analyse the results of centrifuge model tests. The nested yield surface model used in these analyses was developed specifically to model the small-strain non-linearity that is known to characterize the behaviour of clay at small strain. Although these multiple yield surface models produce settlement troughs that are more realistic than those obtained from conventional elasto-plastic models, it seems that further refinements are required to obtain settlement profiles with widths that are consistent with those seen in practice. This tendency of the results of numerical analysis to overpredict the widths of settlement troughs is also discussed by Simpson *et al.* [30], who suggest that models in which the effects of anisotropy of the ground are included may lead to improved results. Further investigation of this suggestion is, however, beyond the scope of this paper.

Figures 12 and 13 provide an interesting comparison because they both relate to the installation of a tunnel in which the characteristics of the liner being modelled are the same. The results in Figure 12, however, were obtained using continuum elements to model the liner (CL) and Figure 13 shows the results of an analysis in which Phaal and Calladine elements are used to model the liner (SL). The computed displacements in Figures 12 and 13 are of a similar shape but quantitatively they are quite different. The settlement trough for the CL analysis, for example, particularly at the end of the analysis (Stage 10) is noticeably deeper and narrower than the settlement trough obtained at the end of run SL. It is clear, then, that the method use to model the

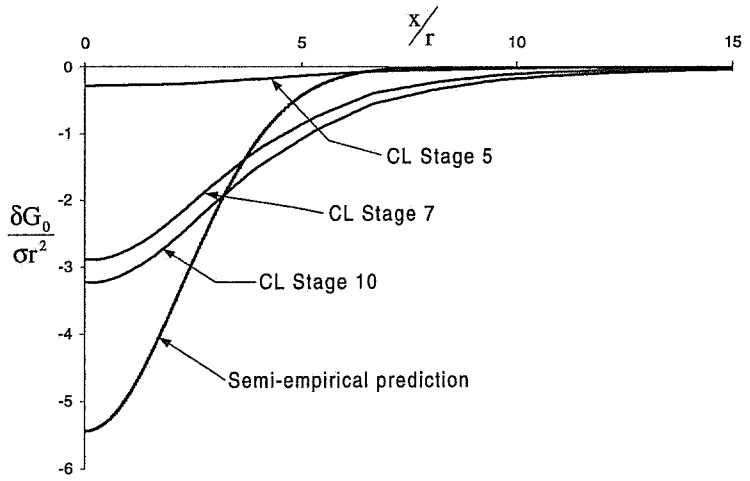

Figure 12. Transverse settlement profile (CL).

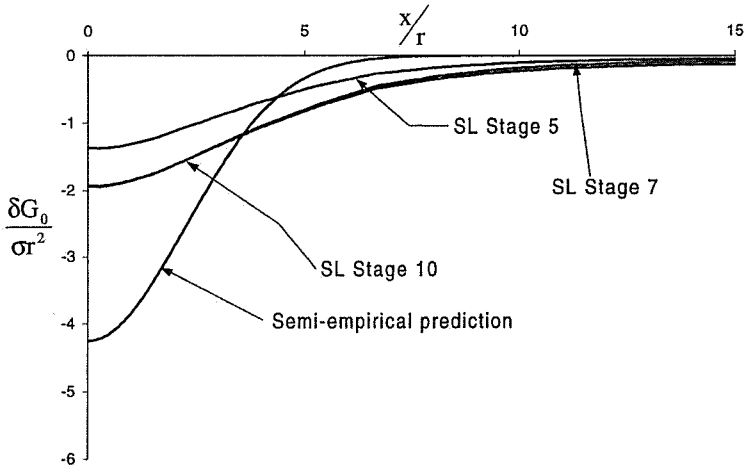

Figure 13. Transverse settlement profile (SL).

tunnel liner can have a significant effect on the nature of the computed surface settlements. A further comparison between the settlements obtained from these two runs is given in Figure 14. These perspective plots show the difference in maximum settlement between the two lining element types that is evident in the two-dimensional plots. The unevenness of the surface settlement profile immediately above the tunnel is probably due to the relatively large (6 m) increments of tunnel installation adopted in these analyses. The unevenness is more pronounced in the shell element analysis although the reason for this behaviour is unclear.

It seems likely the results of run SL are influenced by the over-stiff performance of the embedded Phaal and Calladine elements that was observed in the results of the example analyses described in Section 4. A detailed inspection of the deformed shape of the tunnel at the end of the

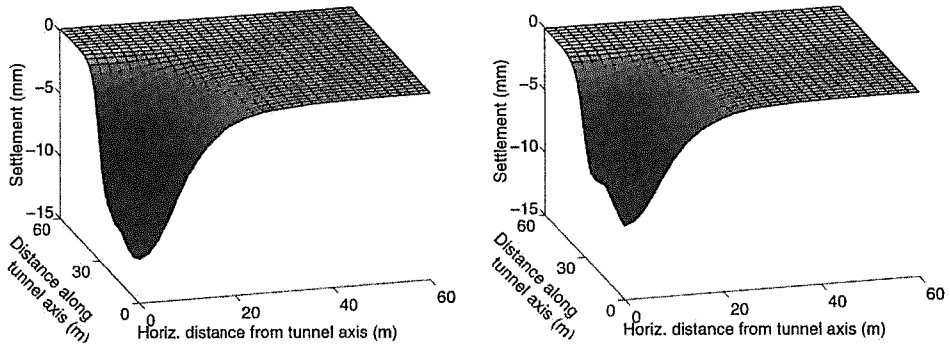

(a) Continuum element liner mesh (analysis CL)

(b) Shell element liner mesh (analysis SL)

Figure 14. 3D perspective plots of settlements with a half complete excavation.

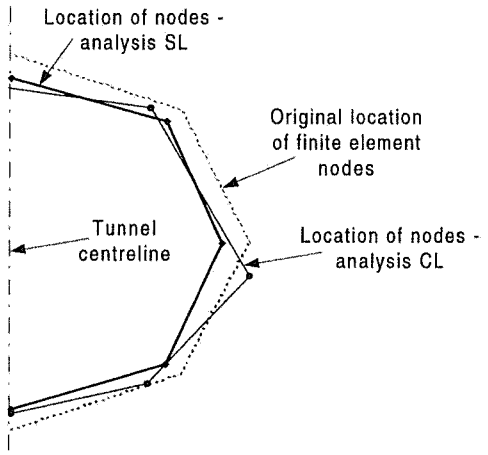

Figure 15. Deformed shape of tunnel at the end of example lined analyses.

analysis shows that the computed deformations of the tunnel cross sections are quite different (see Figure 15). This figure shows the deformations of the element corner nodes magnified by a factor of 20; midside nodes are omitted for clarity. These deformed shapes show that the flexural liner deformations in run SL are significantly less than those in run CL. This difference is presumed to be associated with excessively stiff behaviour of the Phaal and Calladine elements which leads, it is thought, to differences in the computed settlement profiles.

7. CONCLUSIONS

It is clear that considerable care needs to be taken in the choice of numerical formulation and computation procedure to carry out meaningful analysis of stiff embedded tunnel liners. Two

broad approaches appear to be available; the liner may be modelled either using conventional continuum elements or, alternatively, by the use of specially formulated shell elements.

The use of continuum elements to model thin shell structures inevitably leads to elements that have poor geometric conditioning. For the calculations described in this paper, however, it is argued that any consequential round-off errors are not significant provided the computations are based on double precision arithmetic. In this case, thin layers of continuum elements would seem to be a robust procedure for use in practice.

This study suggests that satisfactory results can be obtained when specially formulated shell elements are used to model the tunnel liner. However experience gained using the Phaal and Calladine element suggests that shell elements may behave in an over-stiff manner when embedded in a mesh of continuum elements. This behaviour is presumably associated with a lack of compatibility between the shell and continuum elements and no evidence of over-stiff behaviour is apparent when these shell elements are tested in isolation.

ACKNOWLEDGEMENTS

This work was undertaken with funding from the Engineering and Physical Sciences Research Council. Some calculations were carried out at the Oxford Supercomputing Centre.

REFERENCES

1. Mair RJ, Taylor RN, Burland JB. Prediction of ground movements and assessment of risk of building damage due to bored tunnelling. In *Geotechnical Aspects of Underground Construction in Soft Ground*, Mair RJ, Taylor RN (eds). Balkema: Rotterdam, 1996; 713–718.
2. Augarde CE. Numerical modelling of tunnelling processes for assessment of damage to buildings. *D. Phil. Thesis*, University of Oxford, 1997.
3. Liu G. Numerical modelling of settlement damage to masonry buildings caused by tunnelling. *D.Phil. Thesis*, University of Oxford, 1997.
4. Burd HJ, Houlsby GT, Augarde CE, Liu G. Modelling tunnel-induced settlement of masonry buildings. *Proceedings of ICE Geotechnical Engineering* 2000; **143**:17–29.
5. Gunn M. The prediction of surface settlement profiles due to tunnelling. In *Predictive Soil Mechanics (Proceedings of Wroth Mem. Symposium)*, Schofield A, Houlsby GT (eds). Thomas Telford: London, 1993; 304–317.
6. Addenbrooke T, Potts DM. Twin tunnel construction — ground movements and lining behaviour. In *Geotechnical Aspects of Underground Construction in Soft Ground*, Mair R, Taylor R (eds). Balkema: Rotterdam, 1996; 441–446.
7. Potts DM, Addenbrooke TI. A structure's influence on tunnelling-induced ground movements. *Proceedings of ICE Geotechnical Engineering* 1997; **125**:109–125.
8. Gioda G, Swoboda G. Developments and applications of the numerical analysis of tunnels in continuous media. *International Journal of Numerical and Analytical Methods in Geomechanics* 1999; **23**:1393–1405.
9. Houlsby GT. A model for the variable stiffness of undrained clay. *Proceedings of International Symposium on Pre-Failure Deformation Characteristics of Geomaterials*, Torino, vol. 1. 1999; 443–450.
10. Cook RD, Malkus DS, Plesha ME. *Concepts and Applications of Finite Element Analysis.* (3rd edn). Chichester: Wiley, 1989.
11. Naylor DJ. Filling space with tetrahedra. *International Journal of Numerical Methods in Engineering* 1999; **4**:1383–1395.
12. Neto HL. Numerical conditioning in structural solutions: a proposal for a new condition number. *Advances in Engineering Software* 1994; **19**(3):129–142.
13. Bell RW, Houlsby GT, Burd HJ. Suitability of two and three dimensional finite elements for modelling material incompressibility using exact integration. *Communications in Numerical Methods in Engineering* 1993; **9**(4):313–329.
14. Yang H, Saigal S, Liaw D. Advances of thin shell finite elements and some applications — version 1. *Computers and Structures* 1990; **35**:481–504.

15. Phaal R, Calladine CR. A simple class of finite elements for plate and shell problems. II: An element for, thin shells, with only translational degrees of freedom. *International Journal of Numerical Methods in Engineering* 1992; **35**:979–996.
16. Huang H. *Static and Dynamic Analysis of Plates and Shells.* Springer: Berlin, 1989.
17. Allman D. A compatible triangular element including vertex rotations for plane elasticity analyses. *Computers and Structures* 1984; **19**:1–8.
18. Bergen P, Felippa C. A triangular membrane element with rotational degrees of freedom. *Computer Methods in Applied Mechanics and Engineering* 1985; **50**:25–69.
19. Hughes T, Masud A, Harari I. Numerical assessment of some membrane elements with drilling degrees of freedom. *Computers and Structures* 1995; **55**:297–314.
20. Astley RJ. *Finite Elements in Solids and Structures: An Introduction.* Chapman and Hall: London, 1992.
21. Hibbitt, Karlsson, and Sorensen, Inc., *Abaqus Theory Manual*, Version 5.8, 1998.
22. Zienkiewicz OC, Morgan K. *Finite Elements and Approximation.* Wiley: New York, 1983.
23. Brown P, Booker J. Finite element analysis of excavation. *Computers and Geotechnics* 1985; **1**:207–220.
24. Augarde CE, Burd HJ, Houlsby GT. A three-dimensional finite element model of tunnelling. *Proceedings of NUMOG V*, Davos, Switzerland, 6–8 September, 1995; 457–462.
25. Einstein HH, Schwartz C. Simplified methods for tunnel design. *ASCE Journal of Geotechnical Engineering* 1979; **105**(GT4):499–518.
26. Bakker KJ, Van Scheldt W, Plekkenpol J. Predictions and a monitoring scheme with respect to the boring of the Second Heinenoord Tunnel. In *Geotechnical Aspects of Underground Construction in Soft Ground* Mair R, Taylor R (eds). Balkema: Rotterdam, 1996; 459–464.
27. El-Nahhas F, El-Kadi F, Ahmed A. Interaction of tunnel linings and soft ground. *Tunnelling and Underground Space Technology* 1992; **7**(1):27–31.
28. Rowe RK, Lo KY, Kack GJ. A method of estimating surface settlement above tunnels constructed in soft ground. *Canadian Geotechnical Journal* 1983; **20**:11–22.
29. Stallebrass SE, Grant RJ, Taylor RN. A finite element study of ground movements measured in centrifuge model tests of tunnels. In *Geotechnical Aspects of Underground Construction in Soft Ground*, Mair R, Taylor R (eds). Balkema: Rotterdam, 1996; 595–600.
30. Simpson, B, Atkinson JH, Jovicic V. The influence of anisotropy on calculations of ground settlements above tunnels. In *Geotechnical Aspects of Underground Construction in Soft Ground*, Mair R, Taylor R (eds). Balkema: Rotterdam, 1996; 591–594.

